APPLICATION OF ERS SCATTEROMETER WINDS TO TYPHOON, MONSOON, RAIN, AND EL NINO STUDIES

W.Timothy and Wenqing Tang Jet Propulsion Laboratory 300-323, Pasadena, CA, 91109, U.S.A.
phone:1-818-354-2394, fax:1-818-393-6720

liu pacific.jpl.nasa.gov

http://airsea-www.jpl.nasa.gov

Abstract

The ocean surface wind and pressure derived from the ERS-1 scatterometer, with high spatial resolution, are used to improve the monitoring of the intensity and location of typhoon. The scatterometer winds are used in conjunction with coincident observations of sea surface temperature and precipitable water by other spaceborne sensors to compare the annual and interannual variations of monsoons in the South China Sea and in the Bay of Bengal. The scatterometer data are also used to estimate rain rate through the improved computation of surface wind divergence, vertical velocity profile, and the hydrologic balance in the atmosphere. Finally scatterometer winds, as the forcing or precursor of equatorial Kelvin waves and temperature anomalies, are examined in one of the warming event in the equatorial Pacific.

Keywords: scatterometer, monsoon, storm, rain, El Niño

1. Introduction

The ocean surface is often covered by clouds and spaceborne microwave sensors with their ability to penetrate clouds are ideal instruments to monitor ocean surface parameters. Only an active microwave sensor, the scatterometer, has the proven capability of measuring both wind speed and direction under the widest range of condition. While providing synoptic global view from the vantage point of space, a scatterometer also provides highThe ocean surface is often covered by clouds and spaceborne microwave sensors with their ability to penetrate clouds are ideal instruments to monitor ocean surface parameters. Only an active microwave sensor, the scatterometer, has the proven capability of measuring both wind speed and direction under the widest range of condition. While providing synoptic global view from the vantage point of space, a scatterometer also provides high spatial resolution, unmatched by operational numerical weather prediction (NWP) winds, to study individual weather systems. A spaceborne scatterometer is, perhaps, the only mean of providing observations at adequate ranges of temporal and spatial scales for understanding ocean-atmosphere interaction and global climate and environmental changes. This is a brief summary of a few examples of scientific application of ocean surface winds derived by Freilich and Dunbar [1993], using observations of the scatterometer on the European Remote Sensing Satellite ERS-1.

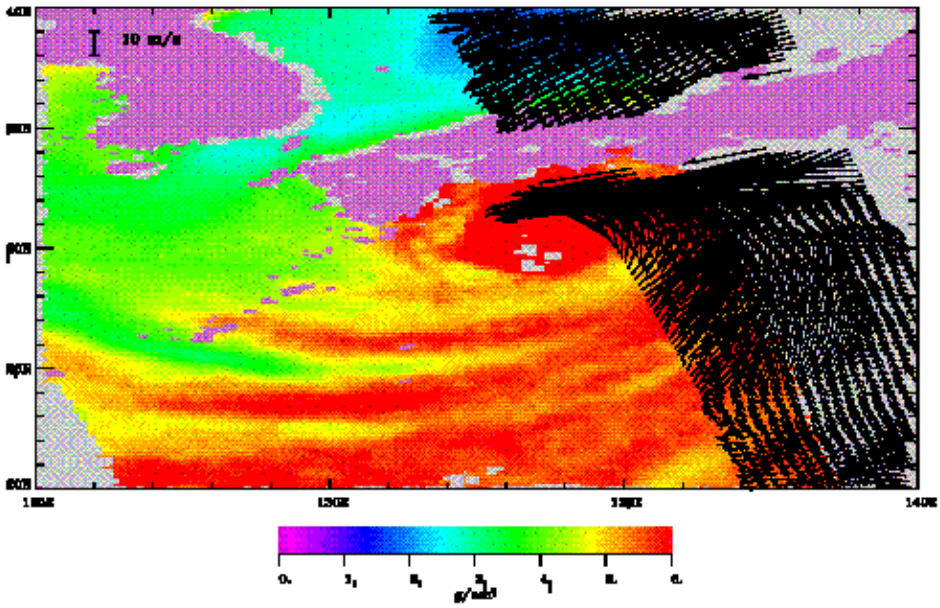

Figure 1. Typhoon Irving is revealed by the wind vectors derived from the ERS-1 scatterometer (dark arrows), the SSM/I precipitable water (color image) as it hits the Honshu Island of Japan on 3 August 1992.

2. Tropical Cyclone

The detailed structure of the wind field within an ERS-1 scatterometer ground track in Fig. 1 illustrates the high spatial resolution (25 km) of the scatterometer. The overlay of scatterometer windson precipitable water from the Special Sensor Microwave / Imager (SSM/I) dramatically visualizes not only the structure of the typhoon, but the relation between the dynamics and the hydrologic balance in the mesoscales. It also demonstrates the "all weather" capabilities of microwave sensors.

Wind observations over ocean are largely made by merchant ships; however, ship reports are sparse, particularly in storms. The spatial resolution of numerical analysis done at weather center are generally insufficient to reveal accurate position and details. Satellite visible and infrared images may help to locate storms but does not reveal the surface intensity. The improvement by spaceborne scatterometer in describing storms have been demonstrated with Seasat data. Surface pressure, which would help to gauge the intensity and to locate the center of the storm, can also be derived from scatterometer winds by inverting a boundary model [Brown and Liu, 1982] assuming geostrophic balance. Such application has been demonstrated in mid-latitude storms [Brown and Levy, 1986]. Hsu and Liu [1996] extended such a technique to study the typhoons (tropical cyclones) by adding a gradient wind balance in deriving pressure field using ERS-1 scatterometer winds. Their results are compared with the operational analysis of the European Center for Medium Range Weather Forecast (ECMWF) in Fig. 2. In the ECMWF analysis, the center of the low pressure is dislocated from the center of the cyclonic flow. The improvement by the scatterometer observations is obvious.

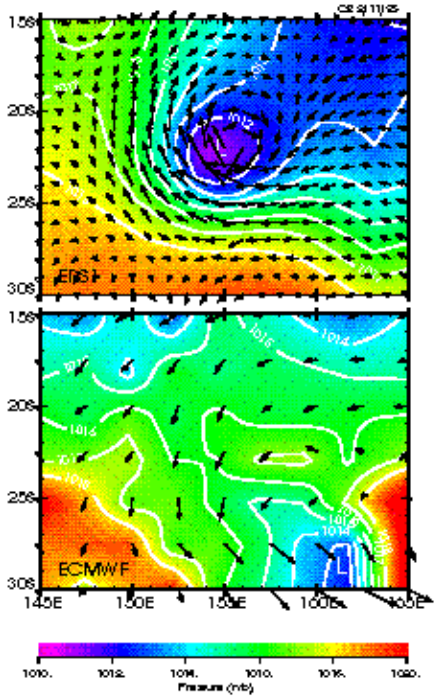

Figure 2. The surface wind vectors (dark arrow) and surface pressure (color image) derived from ERS-1 scatterometer data (upper) and from ECMWF (lower) at 12 UTC, on 11 February 1993, around Tropical Cyclone Olivera.

3. Monsoon

Monsoons are the seasonal changes of winds forced by continent-ocean temperature contrast. Their onset, intensity, and retreat vary greatly, and the variation has strong economic impact and may cause severe human suffering. Over land the consequences of monsoon are, perhaps, well observed, but the breeding ground over the ocean has been insufficiently monitored, and the scatterometer has the potential of making a contribution. The Asian monsoon has a strong influence over 60% of the world's population, yet it is much less studied and understood than the Indian Monsoon.

In Fig. 3, the annual variation of wind speed and direction from ERS-1 scatterometer is compared with the precipitable water from SSM/I and sea surface temperature derived by blending observations of the Advanced Very High Resolution Radiometer (AVHRR) with in situ measurements. In the Bay of Bengal, the wind direction changes gradually from northerly during winter to southwesterly in summer, with moistening of the atmosphere and warming of the ocean. The strength of the wind increases dramatically from June to September, with sharp increase in precipitable water but slight cooling of the ocean. In the South China Sea, there is a much clearer and more dramatic onset of the winter monsoon in late September or early October, with large increase in wind speed, decrease in precipitable water and sea surface temperature. The wind direction changes sharply from south / southwesterly to northeasterly. The onset of summer monsoon appears to be more gradual, over a period from February to April.

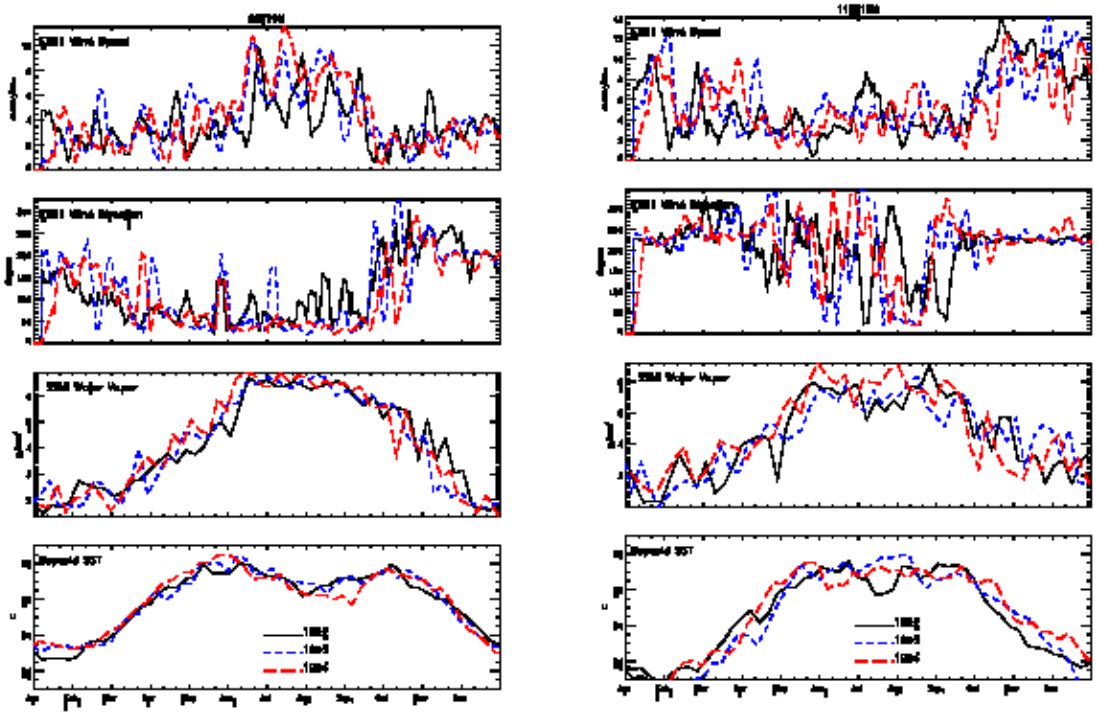

Figure 3. The annual variations of (from top to bottom) wind speed, wind direction, precipitable water, and sea surface temperature for three years, 1992, 1993, and 1994, at two locations, [19°N,90°E] in the Bay of Bengal (left), and at [19°N,115°E] in the South China Sea (right).

4. Rain

The lack of measurements on evaporation (E) and precipitation (P) over ocean has hampered the understanding of the hydrological forcing on the ocean. In the past, the large scale surface water flux (F=E-P) was derived by using the budget method based on the conservation princpal in which F is equated to horizontal divergence of the integrated water vapor transport and the change of water storage in the atmosphere. The computation of integrated water vapor transport requires measurements of the vertical profile of wind vector and humidity in the atmosphere which, traditionally, come from aerological (rawindsonde). Over ocean, even rawindsonde data are sparse and the uniformly gridded outputs from NWP model have been used, with insufficient accuracy and resolution. Since most of the water vapor resides near the surface, the accuracy of lower level winds is expected to outweigh upper level winds in importance. Liu [1993] suggested methods to estimate the hydrologic forcing using a combination of satellite data. Liu and Hsu [1996] and Hsu et al. [1997] have demonstrated that scatterometer winds can be used to improve the computation of surface wind divergence, the vertical velocity profile, the vertical advection of moisture and, therefore, the surface hydrologic forcing, particularly over convective areas.

On January 17 and 23, 1993, the ERS-1 scatterometer passed over a 10° latitude by 10° longitude experiment area shown in Fig. 4. On January 17, the rain map derived from observations by the Japanese Geostationary Meteorological Satellite (GMS) shows maxima lying in a northwest to southeast axis (lower left), but the hydrologic forcing computed using ECMWF data alone (upper left) shows a large maximum lying on the equator with no northwest to southeast trend, and a zonally oriented high rain area at 3°S. With the addition of scatterometer winds, the pattern of the computed hydrologic forcing (center left) becomes much closer to the rain maps; maxima appear along the northwest to southeast axis. On January 23, the GMS rain map (lower, right) shows rainfall decreases from north to south, with high values appear largely north of the equator. The hydrologic forcing computed from ECMWF data alone shows rainfall decreases from west to east, with high values east of 154°E. The addition of scatterometer winds again brings the patterns of hydrologic forcing closer to the rain map. In these comparisons, the variation of evaporation over the area is assumed to be small.

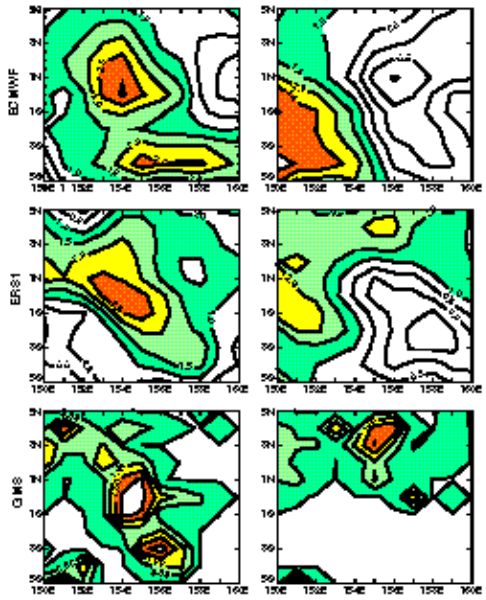

Figure 4. Hydrologic forcing computed from ECMWF data alone (upper) and with ERS-1 scatterometer winds replacing the ECMWF surface winds (center); and the GMS rain rate, for 17 January 1993 (left) and 23 January 1993 (right).

5. El Niño

The evolution of an El Niño warming event in the eastern tropical Pacific at the second half of 1994 was inferred from sea-level rise measured over several months by the microwave altimeter on the Topex/Poseidon spacecraft [Space News, Vol. 6, No. 5, page 13, 1995]. Part of this warming events was examined by Liu et al. [1995] using a combination of satellite data and ocean general circulation model. In Fig. 5, three spaceborne sensors were combined to describe this event. The deviations of the 1994-1995 values of a parameter from its corresponding values in the previous years are shown and these deviations are, hereafter, referred to as anomalies. In the equatorial eastern Pacific, the Trades Winds generally blow from the west to the east and their zonal components are negative. During the second half of 1994, four distinct groups of equatorial westerly (positive) wind anomalies were observed by the scatterometer on ERS1 to occur near the date line. Each group of wind anomalies initiated an eastward-propagating, downwelling Kelvin wave that was exhibited as anomalous sea-level rise observed by Topex/Poseidon altimeter.

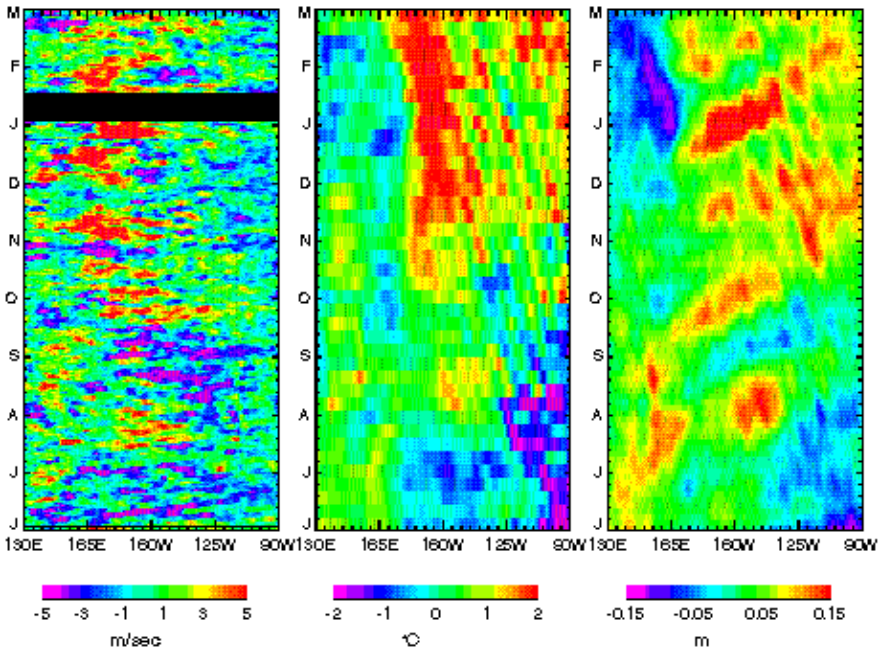

Figure 5. Time-longitude variation, along the equator, of the deviation of the 1994-1995 values from the values in the previous years, for ERS-1 zonal wind (left), blended sea surface temperature (center), Topex/Poseidon sea level (right).

The strength of the wave increases from September to December 1994, but then It is obvious that this anomalous warming event is not continuous, but consists of a series of intraseasonal episodes. Unlike the El Niño events of the 1980s, equatorial warming events in the 1990s are more frequent, last for shorter periods, and are less intense. Whether the 1994 warming can be classified as an El Niño is being debated. The coincident observations infer clearly that the westerly wind anomalies are precursor of equatorial warming. El Niño has been perceived as a interannul climate signal, but the equatorial warming events appears to have

a decadal trend and may respond to intra-seasonal forcing. The predictability of seasonal-to-interannual changes may lie in our understanding of the shorter and longer time-scale variabilities and our ability to monitor them.

Acknowledgments

This study was performed at the Jet Propulsion Laboratory, California Institute of Technology, under contract with the National Aeronautic and Space Administrations (NASA). It was supported by NASA Scatterometer (NSCAT) and Earth Observing System (EOS) Projects. We are grateful to Frank Wentz for providing the SSM/I data.

References

Brown, R.A., and W.T. Liu, 1982:
An operational large-scale marine boundary layer model. *J. Appl. Meteor.*, **21**, pp. 261-269.

Brown, R.A., and G. Levy, 1986:
Ocean surface pressure fields from satellite sensed winds. *Mon. Wea. Rev.*,**114**, pp. 2197-2206.

Freilich, M.H., and R.S., Dunbar, 1993:
A preliminary C-band model function for the ERS-1 AMI instrument. *Proc. First ERS-1 Symposium , ESP SP-359.*, 79-84.

Hsu, C.S. and W.T. Liu, 1996:
Surface wind and pressure field near tropical cyclone Oliver derived from ERS-1 scatterometer observation. *J. Geophys. Res.*, **101**, pp. 17,021-17,027.

Hsu, C.S., W.T. Liu, and M.G. Wurtele, 1997:
Impact of scatteromometer winds on hydrologic forcing and convective heating through surface divergence. *Mon. Wea. Rev.*, submitted.

Liu, W.T., 1993:
Ocean Surface Evaporation. Atlas of Satellite Observations Related to Global Change. R.J. Gurney, J. Foster, and C. Parkinson (eds.), Cambridge University Press, Cambridge, 265-278.

Liu, W.T., and C.S. Hsu, 1996:
Surface wind divergence, convective transport, and hydrologic forcing on the ocean. *Preprint Vol., Eighth Conf. Air-sea Interaction.* Amer. Meteorol. Soc., Boston, pp. 68-72.

Liu, W.T., W. Tang, and L.L. Fu, 1995:
Recent Warming Event in the Pacific May Be an El Niño. *Eos Trans of Amer. Geophys. Union*, **76** No. 43, pp. 429-437.